Journal of Alloys and Compounds 506 (2010) 541–547

Contents lists available at ScienceDirect

Journal of Alloys and Compounds

journal homepage: www.elsevier.com/locate/jallcom

Synthesis, characterization and physicochemical properties of nanosized Zn/Mn oxides system

M.M. Selim[a], N.M. Deraz[a,b], O.I. Elshafey[a,*], A.A. El-Asmy[c]

[a] Physical Chemistry Department, Laboratory of Surface Chemistry and Catalysis, National Research Center, Dokki, Cairo, Egypt
[b] Chemistry Department, College of Science, King Saud University, P.O. Box 2455, Riyadh 11451, Saudi Arabia
[c] Chemistry Department, Faculty of Science, El-Mansoura University, Mansoura, Egypt

ARTICLE INFO

Article history:
Received 4 February 2010
Received in revised form 4 April 2010
Accepted 25 April 2010
Available online 5 May 2010

Keywords:
Zinc oxide
Manganese oxide
Li_2O doping
Zinc manganite
Catalytic activity

ABSTRACT

A series of pure and doped Li_2O–zinc/manganese mixed oxides was prepared by ceramic route at 400–1000 °C. The obtained solids have been characterized by the thermo-gravimetric analyzer (TGA), differential scanning calorimetry (DSC), X-ray powder diffractogram (XRD), infrared (IR), transmission electron microscopy (TEM) and energy dispersive X-ray (EDX) techniques. The catalytic behavior of pure and doped mixed solids was investigated using the decomposition reaction of H_2O_2 at 30–50 °C. The obtained results revealed that the solid state reaction between ZnO and Mn_2O_3 started at 500 °C yielding zinc manganite ($ZnMn_2O_4$) nanoparticles. The augmentation in the calcination temperature of the investigated solids up to 1000 °C for 4 h brought about complete conversion of unreacted oxides yielding $ZnMn_2O_4$ crystallites. By doping the system with Li_2O at different calcination temperatures, an enhancement of the formation of zinc manganite was observed. The products obtained by doping with Li_2O at different temperatures had less catalytic activity than the pure solids. The catalytic activity of pure and Li_2O-doped Zn/Mn mixed oxides system decreased by increasing the calcination temperature.

1. Introduction

Most divalent metal oxides (MO) interact with Mn_2O_3 yielding the corresponding manganite with formula MMn_2O_4 having the spinel-like structure. There are of particular interest owing to the attractive possibility of replacing cations in tetrahedral and octahedral sites available in their crystal lattices. These mixed oxides have many applications in several fields related to adsorption, refractory, catalysis and solid state [1–3]. The performance of mixed oxides in various applications depends on the nature of the individual oxides [4], their respective ratios, thermal treatment [1,5–8], preparation technique [6] and the doping with some foreign cations such as Li^+, Ag^+, Mg^{2+} and Zn^{2+} [6,9–14].

The enhancement of formation of spinel compounds, due to doping, had been attributed to the effective increase in the mobility of reacting cations taking part in the manganite formation [6,9–14]. The interesting physical and chemical properties of spinel manganite arise from the distribution of transition metal cations having various oxidation states, among the available tetrahedral and octahedral sites [4]. The activity of pure and doped manganese based systems towards H_2O_2 decomposition was previously studied [12–15]. There were unique features associated with Li_2O that are of interest. The Li_2O doping favored the dispersion of manganese oxide on the surface of doped $L_1Z_1M_2$ catalyst calcined at 400 °C brought about an increase in the catalytic activity of mixed oxides. Sometimes it decreases the catalytic activity of manganese oxides [12]. No measurable activity as observed for samples precalcined at 1000 °C because of the formation of inactive compounds and/or sintering process. The changes in the catalytic activity of pure and doped solids were attributed to the change in oxidation states from Mn^{4+} to Mn^{2+} on increasing the calcination temperature.

Pretreatments did not modify the mechanism of the catalyzed reaction but changed the number of catalytically active sites without changing the nature of these sites.

The present work describes the effects of Li_2O doping and calcination temperature on the physicochemical and catalytic properties of Zn/Mn mixed oxides system prepared by mechanical ceramic method. The techniques employed were XRD, EDX, IR, DSC, TEM and H_2O_2 decomposition at 30–50 °C.

2. Experimental

2.1. Materials

The chemicals employed in the present work were of analytical grade supplied by Fluka Company. Pure zinc–manganese mixed oxide solids having the ratio of 1:2 were prepared by mechanical mixing of known amounts of basic zinc carbonate

* Corresponding author. Tel.: +20190404856; fax: +20233370931.
E-mail address: olalolo2004@yahoo.com (O.I. Elshafey).

0925-8388/$ – see front matter © 2010 Published by Elsevier B.V.
doi:10.1016/j.jallcom.2010.04.180

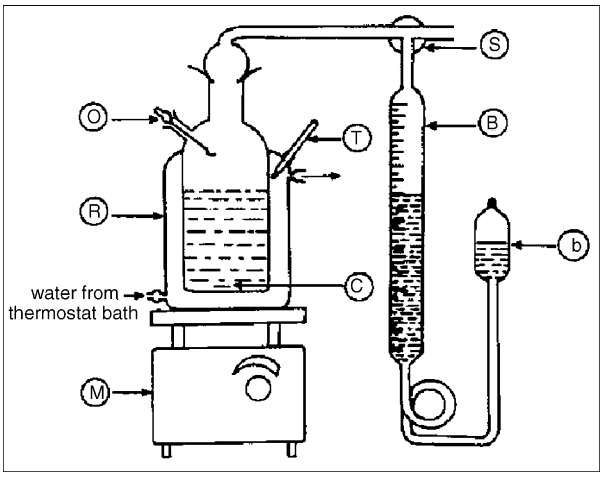

Fig. 1. Apparatus for studying the kinetics of the decomposition of H_2O_2.

and $MnCO_3$ and then subjected to thermal treatment in air at 400, 500, 700, 800 and 1000 °C for 4 h. The symbol of the prepared calcined mixed solid is designated as Z_1M_2. Doped Li_2O–Zn/Mn oxide samples were obtained by impregnating specified amounts of Zn and Mn carbonates with different amounts of lithium nitrate dissolved in the least amount of distilled water. The obtained paste was dried at 100 °C and calcined at the previous temperatures. The concentrations of Li_2O were 1 and 4 mol% Li_2O can be designated as $L_1Z_1M_2$ and $L_4Z_1M_2$, respectively.

2.2. Techniques and calculations

Energy dispersive X-ray, EDX, measurements were carried out on a Hitachi S-800 electron microscope with a Kevex Delta system attached. The parameters were: −15 kV accelerates voltage, 100 s accumulation time and 8 μm windows width. The surface molar composition was determined by the Asa method (Zaf-correction, Gaussian approximation).

X-ray powder diffractograms, XRD, of the samples calcined at 400, 500, 700, 800 and 1000 °C for 4 h were recorded using a Bruker diffractometer (Bruker D8 advance target) and the scan rate was fixed at 8° in 2θ min^{-1} for phase identification. The patterns were run with Cu K_α with secondly monochromator (λ = 0.1545 nm) at 40 kV and 40 mA. The crystallite size of crystalline phases of different investigated solids was calculated from the line broadening of the main diffraction lines of these phases using Scherrer's equation [16]:

$$d = \frac{B\lambda}{\beta \cos\theta}$$

where d is the mean crystallite diameter, λ is the X-ray wave length, B is the Scherrer constant (0.89), β is the full-width at half-maximum (FWHM) of the main diffraction peak of crystalline phases and θ is the diffraction angle.

The infrared (IR) spectra of the various solids calcined at different temperatures was recorded using Perkin-Elmer Spectrophotometer (1430) at 4000–400 cm^{-1}. The sample disks were placed in the holder of the double grating IR spectrometer [17].

Transmission electron microscope (TEM) observation was performed on a JEOL JEM-1230 electron microscope at accelerating voltage of 120 kV. TEM samples were deposited on thin amorphous carbon films supported on copper grids from ultrasonically processed ethylene glycol solution of the products and used to observe the morphology of the nanosized particles. A drop of the solution was placed on a copper grid that was left to dry before transferring into the TEM sample chamber.

Differential scanning calorimetry (DSC) of the samples was carried out using SETARAM thermal analysis apparatus with flow rate of argon 30 ml min^{-1}. The rate of heating was kept at 10 °C/min and the mass of sample was 50 mg. Thermogravimetry (TG) was carried out using Perkin-Elmer thermo-gravimetric analyzer, the rate of heating was kept at 20 °C min^{-1}. An 18 mg sample of solid specimen was used in each case.

The decomposition of H_2O_2 was followed by measuring the volume of oxygen evolved by using gasometric apparatus (Fig. 1) which consists of a jacketed glass reactor (R); connected by a PVC tubing to the gas burette (B) through a three-way stopcocks (S) [18]. C-magnetic peddle (glass coated); M-magnetic stirrer; T-thermometer. The gas burette was connected from bottom to leveling bulb (b) by a long flexible rubber tubing. The manometric liquid was water containing 5% NaCl and saturated with oxygen to prevent the dissolution of any librated oxygen. The neck of the reactor has a provision to add a known weight of the catalyst sample through the outlet (O) by turning the spoon upside down. For each of the investigated samples a mass of 200 mg was taken for each catalytic run. For each of the investigated samples a mass of 200 mg was taken for each catalytic run.

For each of the investigated samples a mass of 200 mg was taken for each catalytic run. The rate of the decomposition H_2O_2 was determined at three different temperatures 30, 40 and 50 °C. The actual change in the concentration during the catalytic run was determined from the following formula.

$$C = C_o - \frac{PV_g}{RTV_1}$$

where C: concentration of H_2O_2 at time t, in mol L^{-1}, C_o: initial concentration of H_2O_2, in mol L^{-1}, P: atmospheric pressure (1 atm), V_g: volume of the gas librated at time t, in ml, V_1: total volume of solution, in ml, T: temperature, in K, R: gas constant, 0.082051 L atm K^{-1}.

3. Results

3.1. XRD analysis

The X-ray diffractograms of pure Z_1M_2 and doped $L_1Z_1M_2$ mixed oxides system calcined at 400, 500, 700, 800 and 1000 °C are given in Fig. 2(A) and (B). Fig. 2(A) reveals the following: (i) the mixed solids calcined at 400 °C consisted of very small crystal of ZnO as well as MnO_2 γ-MnO_2. (ii) The rise in the calcination temperature to 500 °C resulted in conversion of MnO_2 to Mn_2O_3 with subsequent crystallization of ZnO phase and the appearance of $ZnMn_2O_4$ [19,20]. In addition, increasing the heat temperature from 700 to 800 °C brought about an increase in the peak height

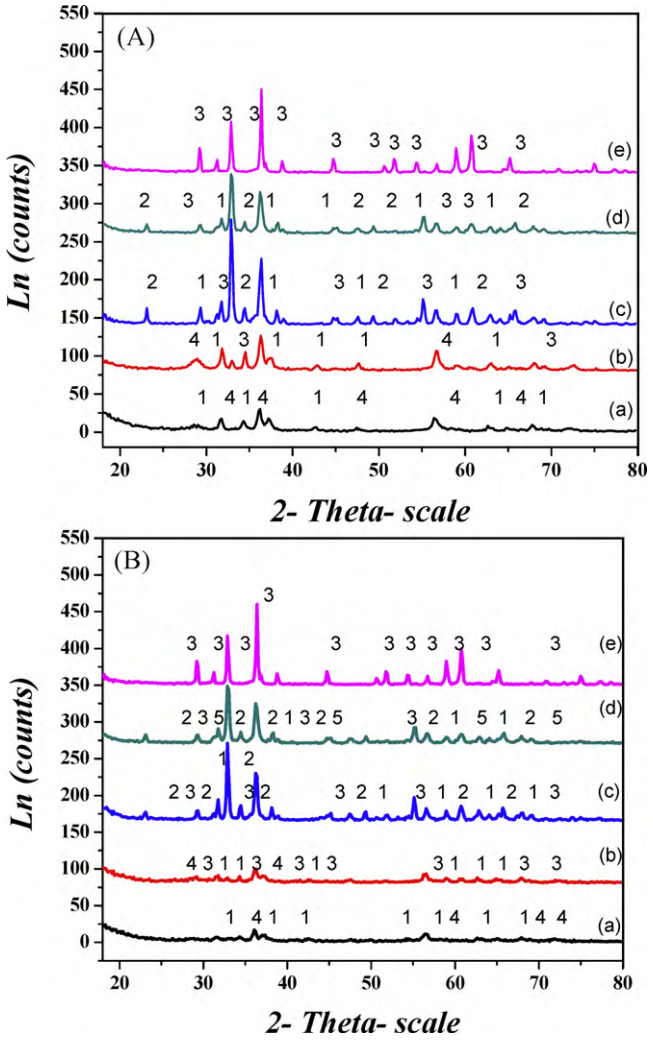

Fig. 2. The X-ray diffraction pattern of (A) Zn/Mn pure (1:2) and (B) doped 4 mol% LiO_2 Zn:Mn (1:2) mixed oxides calcined at calcined at (a) 400 °C, (b) 500 °C, (c) 700 °C, (d) 800 °C and (e) 1000 °C.

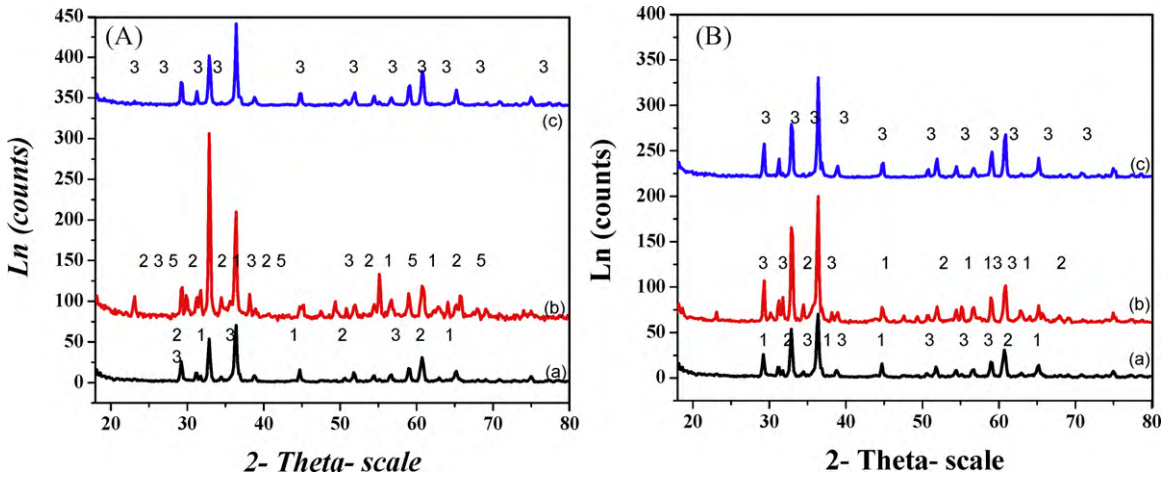

Fig. 3. The X-ray diffraction pattern of (A) Zn:Mn pure (1:2) and (B) doped 4 mol% LiO_2 Zn/Mn (1:2) mixed oxides calcined at 800 °C for (a) 2 h, (b) 4 h and (c) 8 h.

of $ZnMn_2O_4$ phase with subsequent decrease in that of ZnO and MnO species. (iii) The mixed solids calcined at 1000 °C for 4 h consisted of $ZnMn_2O_4$ crystals as a single phase. (iv) Treating Zn/Mn mixed oxide with small amount of Li_2O and treated at 400, 500, 700 and 800 °C indicated that at 400 and 500 °C did not include any new phases. Increasing the calcination temperature of the investigated mixed solids from 700 to 800 °C led to an increase in the intensity of the lines characteristic for $ZnMn_2O_4$ and the appearance of new diffraction lines at d = 1.52 and 2.01 Å corresponding to $Li_4ZnMn_3O_8$. The appearance of $Li_4ZnMn_3O_8$ phase could be tentatively attributed to the solid–solid interaction between Li_2O and ZnO and Mn_2O_3 oxides. Calcination at 1000 °C gave only $ZnMn_2O_4$ lines. (v) The effects of time of calcination on the phase structure of pure and 4 mol % Li_2O–Zn/Mn mixed oxides system were determined and illustrated in Fig. 3(A) and (B). The mixed solids calcined at 800 °C for 2 h are sufficient to form $ZnMn_2O_4$ which appeared with ZnO and Mn_2O_3. However, the calcination of the investigated solids for 4 h led to an increase in the degree of crystanillity of $ZnMn_2O_4$ and decrease in the degree of crystanillity of the rest phases with the formation of Mn_3O_4 phase. Further increase in the time of calcination temperature of the investigated solids for 8 h to complete conversion to $ZnMn_2O_4$ is noticed with a measurable increase in the crystallite size of $ZnMn_2O_4$ phase. The effect of calcination temperature, doping and time of calcination temperature on the degree of crystallinity and crystallite size of MO, ZnO and $ZnMn_2O_4$ phases are given in Tables 1 and 2.

Table 1
Effect of calcination temperature on crystallite size and degree of crystallinity for pure Z_1M_2 mixed oxide.

Calcination temperature (°C)	Time of calcination, h	Phases	Degree of crystallinity (a.u.)[a]	Crystallite size (nm)
400	4	ZnO	31.5	22.4
		MnO_2	15.8	12.4
500	4	ZnO	48.6	25.5
		Mn_2O_3	18.6	20.4
		$ZnMn_2O_4$	13.3	58.5
700	4	ZnO	92.6	35.8
		Mn_2O_3	176	62.4
			24.8	66.9
800	4	ZnO	27.6	34.9
		Mn_2O_3	25.2	41.5
		$ZnMn_2O_4$	34.3	42.1
800	2	ZnO	48.0	76.9
		Mn_2O_3	31.5	67.6
		$ZnMn_2O_4$	78.0	77.6
800	8	$ZnMn_2O_4$	106.0	85.6
1000	4	$ZnMn_2O_4$	114.0	88.3

[a] The peak area of the main diffraction line was considered as a quantitative measure for the degree of crystallinity of the phase present.

Table 2
Effect of calcination temperature and doping with 4 mol% Li_2O on crystallite size and degree of crystallinity for doped Z_1M_2–Li_4 mixed oxide.

Calcination temperature (°C)	Time of calcination, h	Phases	Degree of crystallinity (a.u.)*	Crystallite size (nm)
400	4	ZnO	16.60	32.9
		MnO_2	10.10	20.2
500	4	ZnO	20.0	23.4
		MnO_2	9.10	29.0
		$ZnMn_2O_4$	8.32	63.2
700	4	ZnO	75.00	34.3
		Mn_2O_3	118.00	65.3
		$ZnMn_2O_4$	17.80	79.0
		$Li_4ZnMn_3O_8$	23.30	54.8
800	2	ZnO	15.80	70.8
		$ZnMn_2O_4$	38.80	40.9
800	4	ZnO	53.00	52.9
		Mn_2O_3	141.00	76.7
		$ZnMn_2O_4$	78.80	91.6
		$Li_4ZnMn_3O_8$	20.80	46.7
800	8	$ZnMn_2O_4$	118.00	61.6
1000	4	$ZnMn_2O_4$	178.00	99.7

a* arbitrary unit.

3.2. EDX investigation

EDX investigation of Zn and Mn oxides with ratio 1:2 system prepared by mechanical mixing method was carried out.

Inspection of Table 3 shows the following:

(1) The surface atomic Zn/Mn ratio in the solid prepared by mechanical mixing method and calcined at 600, 800 and 1000 °C is strongly dependent on the calcination temperature.
(2) The surface concentration of Mn in all solids is higher than that in the bulk of solids. On the other hand, surface zinc concentration is smaller than that present in the bulk of different solids.
(3) For pure Zn/Mn mixed oxides system calcined at 600, 800 and 1000 °C, the increase in calcination temperature from 600 to

Table 3
The relative atomic abundance of pure Z_1M_2 and doped $L_4Z_1M_2$ mixed oxide present in the upper most surface layers of different solids investigated.

Temperature (°C)	Atomic abundance							
	Pure Z_1M_2 mixed oxide				Doped $L_4Z_1M_2$ mixed oxide			
	Mn %	Zn %	O%	Surface Mn/Zn ratio	Mn %	Zn %	O%	Surface Mn/Zn ratio
400	75.2	12.1	14.7	6.2	59.2	20.6	14.1	2.8
600	68.6	16.6	27.6	4.1	66.8	17	16.6	3.9
800	66.6	18.6	12.7	3.5	67.9	18	20.2	3.7
1000	51.7	20.6	14.8	2.5	69.8	13.5	16.2	5.1

The relative atomic abundance of Zn/Mn species present in the upper most surface layers of different solids investigated is given.

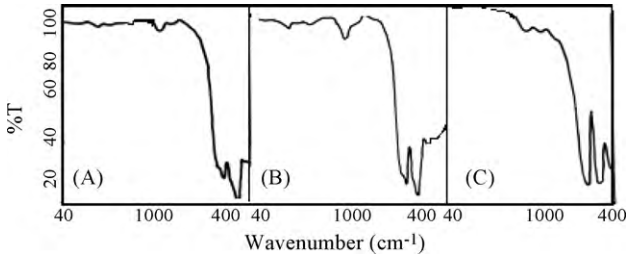

Fig. 4. FTIR spectra for pure Zn/Mn oxides calcined at (a) 600 °C, (b) 800 °C and (c) 1000 °C.

1000 °C resulted in an effective diffusion of manganese species from the surface of the solids towards their bulk and a significant increase in surface concentration of zinc species which decreased from 12.1 to 20.6 at.% and from 75.2 to 51.7 at.% for manganese species. This finding is expected because of the concentration gradient of manganese and zinc between bulk and surface of the solids investigated.

(4) The addition of 4 mol% Li_2O for the specimen and treated at 600–1000 °C resulted in a significant increase in surface concentration of manganese species which increased from 59.2 to 69.8 atom % and migration of free zinc atom from the surface to the bulk from 20.6 to 13.5 atom %.

3.3. Infrared spectra

The IR spectra of the prepared samples treated at 600, 800 and 1000 °C are presented in Fig. 4. The spectrum of pure Z_1M_2 oxide calcined at 600 °C shows a strong bands at 512 and 619 cm^{-1} with a weak one at 412 cm^{-1} related to $ZnMn_2O_4$ spinel. Increasing the treatment temperature to 800 °C, The bands appear more intense and strong due to the formed spinel has more ordered crystals. At 1000 °C, the bands are shifted to higher wavenumbers appearing at 545, 641 and 423 cm^{-1} indicating that the sample becomes well ordered indicating the formation of Zn manganite crystalline spinel.

3.4. Morphology studies

Transmission electron micrographs (Fig. 5a–c) of pure mixed solids followed by calcination at 400, 600 and 800 °C consisted of agglomerated spherical grains with visible grain boundaries and the average grain size of 36, 79 and 88 nm. The treated samples with $L_4Z_1M_2$ at 400, 600 and 800 °C are shown in Fig. 5d–f. It can be seen from the figure that the Li_2O-doping process led to a significant increase in the particle size of the investigated solids from 45 to 114 nm. This process plays important role in the production of nanosized particles.

3.5. DSC and TG studies

The differential scanning calorimetry analysis, DSC, curves of pure Z_1M_2 and treated $L_4Z_1M_2$ oxides are given in Fig. 6. Four sets of endothermic peaks were observed located at 8–103, 190–290, 350–450 and 600–800 °C. The first and fourth sets of peaks are broad and weak, but the second and third sets are sharp and strong.

The thermo-gravimetric, TG and DTG, curves of the pure and treated are given in Fig. 7. The curves consist of two distinct pro-

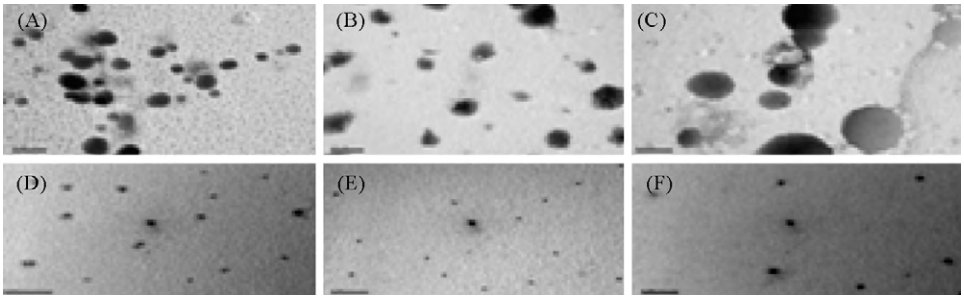

Fig. 5. TEM spectra for pure Zn/Mn oxide calcined at 400 °C (a), 600 °C (b) and 800 °C (C). And for Li_2O-doped mixed solids (d) 400 °C, (e) 600 °C and (f) 800 °C.

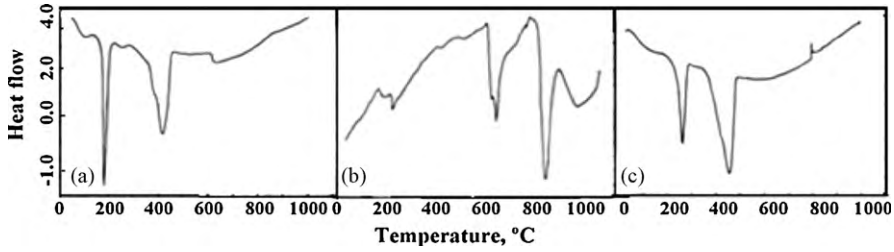

Fig. 6. DSC spectra for (a) pure Zn/Mn oxide, (b) 1 mol% doped Li_2O–Zn/Mn oxide mixed solids and (c) 4 mol% doped Li_2O–Zn/Mn oxide mixed solids.

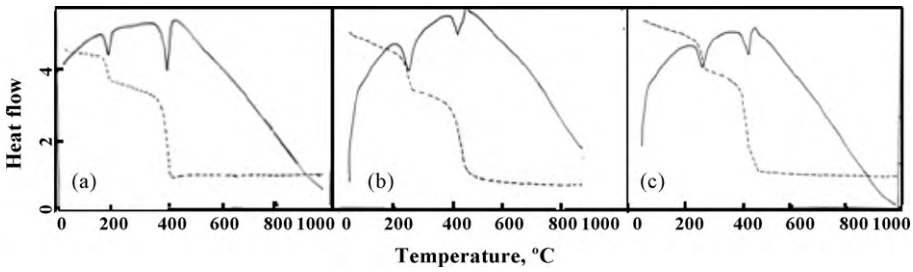

Fig. 7. DSC–TGA spectra for (a) pure Zn/Mn oxide, (b) 1 mol% doped Li_2O–Zn/Mn oxide mixed solids and (c) 4 mol% doped Li_2O–Zn/Mn oxide mixed solids.

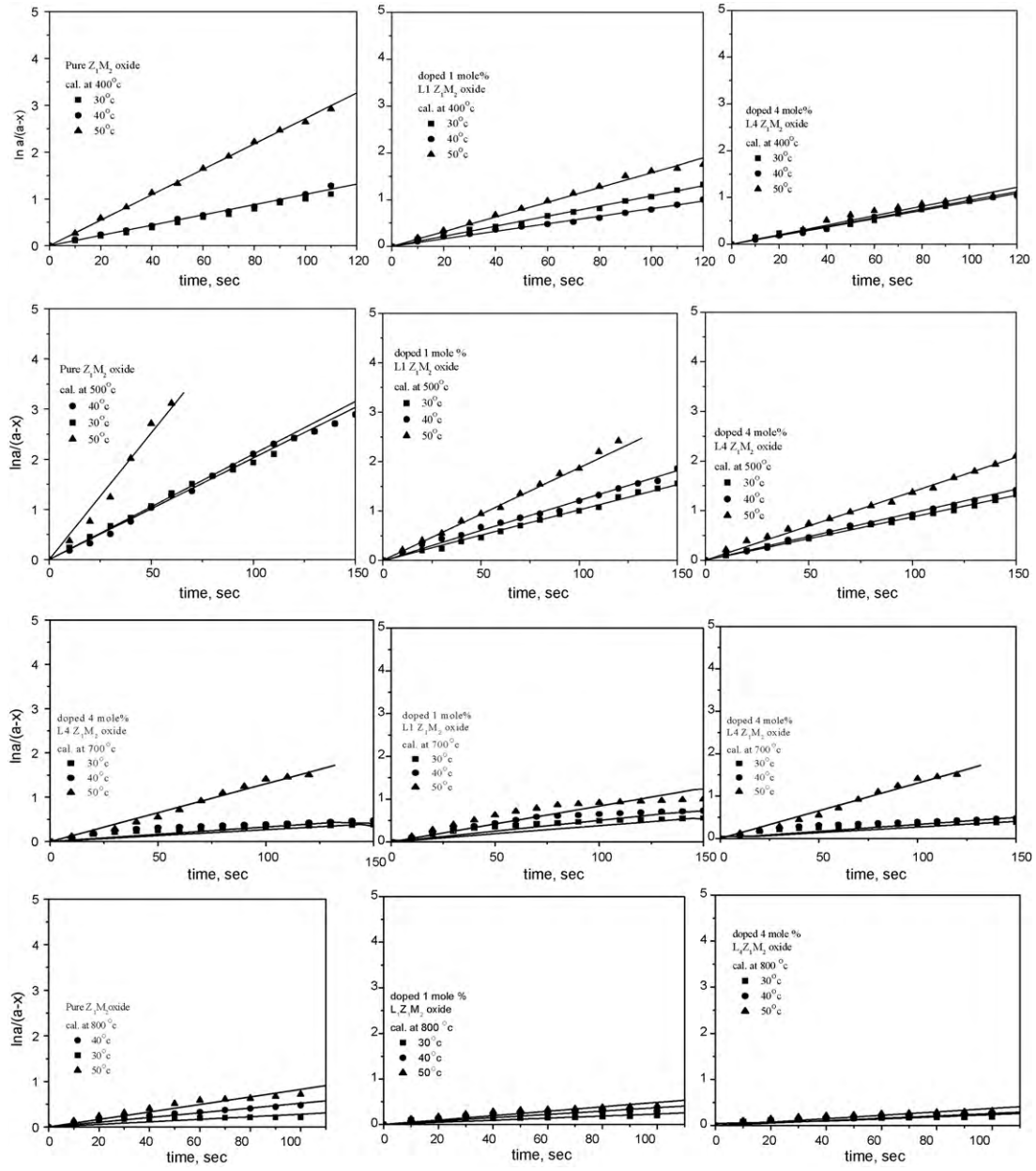

Fig. 8. (a) First order plots for the catalytic H_2O_2 decomposition at three different temperatures (30–50 °C) for the decomposition of H_2O_2 over 0.025 g of pure Zn/Mn (1:2), doped 1 and 4 mol% mixed oxides calcined at 400 °C. (b) First order plots for the catalytic H_2O_2 decomposition at three different temperatures (30–50 °C) for the decomposition of H_2O_2 over 0.025 g of pure Zn/Mn (1:2), doped 1 and 4 mol% mixed oxides calcined at 500 °C. (c) First order plots for the catalytic H_2O_2 decomposition at three different temperatures (30–50 °C) for the decomposition of H_2O_2 over 0.025 g of pure Zn/Mn (1:2), doped 1 and 4 mol% mixed oxides calcined at 700 °C. (d) First order plots for the catalytic H_2O_2 decomposition at three different temperatures (30–50 °C) for the decomposition of H_2O_2 over 0.025 g of pure Zn/Mn (1:2), doped 1 and 4 mol% mixed oxides calcined at 800 °C.

cesses occurring at 261 and 433.5 °C accompanied by mass losses of 10.77% (Calcd. 9.4%) and 21.8% (Calcd. 24%).

3.6. Catalytic activity

The catalytic activity of pure Z_1M_2; doped $L_1Z_1M_2$ and $L_4Z_1M_2$ mixed oxides, precalcined at 400, 600 and 800 °C was tested in the decomposition of hydrogen peroxide in aqueous solution at 30, 40 and 50 °C. The decomposition kinetics of hydrogen peroxide in the presence of the samples was found to follow first order mechanism with respect to H_2O_2. Thus, plots of $\ln(a/a-x)$ versus t were linear over about 80% of the total reaction time Fig. 8(a–d). The catalytic activity of the studied samples could be expressed in terms of rate constants per unit mass of the catalyst. The values of reaction rate constant (K, min^{-1}) of the catalyzed reaction carried out at a given temperatures were calculated and listed in Table 5. Li_2O-doped mixed oxide samples were found to have catalytic activity less than those without lithium.

4. Discussion

4.1. XRD analysis

The X-ray diffractograms of pure Z_1M_2 and doped $L_1Z_1M_2$ and $L_4Z_1M_2$ mixed oxides calcined at 400 °C in Fig. 2(A) and (B). The diffractogram revealed that 400 °C not sufficient for the solid state reaction to occur between ZnO and Mn_2O_3 yielding $ZnMn_2O_4$. Increasing the heat temperature from 500 to 800 °C brought about an increase in the peak height of $ZnMn_2O_4$ phase with a subsequent decrease in that of Zn and Mn oxides. Increasing the calcination temperature of different solids from 400 to 1000 °C led to a measurable increase in both crystallite size and degree of crystallinity of $ZnMn_2O_4$ phase. This finding indicates clearly the thermal stability of the produced $ZnMn_2O_4$ phase even by heating at 1000 °C. It can be concluded that the increase in the calcination temperature causes a gradual crystallization of the spinel phase $ZnMn_2O_4$ with more ordered arrangement of atoms. Treating the mixed solid with small amount of Li_2O for the specimen and treated at 600–1000 °C, enhance the degree of crystallinity and increase the crystallite size of $ZnMn_2O_4$ phase. This may be due to dissolution of lithium species in the single manganite crystallites with subsequent contraction of lattice dimensions indicating the formation of nanosized zinc manganite [21]. The fact that the amount of Li_2O added is far below the detection limit of X-ray diffractometer points out to the enriched presence of the dopant agent in the top surface layers of doped solids. The increase in the time of calcination at 800 °C from 2 to 8 h led to a significant increase in the crystallite size of $ZnMn_2O_4$ phase indicating an effective sintering of the manganite phase.

4.2. EDX investigation

The EDX data for pure Z_1M_2 and doped $L_1Z_1M_2$ and $L_4Z_1M_2$ mixed oxides and treated at 600, 800 and 1000 °C indicated that:

(1) For pure Zn/Mn mixed oxides calcined at 600, 800 and 1000 °C, the diffusion of manganese species occurs from the surface to the bulk. The decrease of manganese on the surface results from the enriched Mn species on the top surface layers. The increase in surface concentration of zinc species is expected because of the concentration gradient of manganese and zinc between bulk and surface of the investigated solids.
(2) The opposite effect due to treating the mixed solid with small amount of Li_2O for the specimen and treated at 600–1000 °C, is attributed to the creation of anionic vacancies in the matrix of transition metal oxides creating vacancies which might prevent the aggregation of manganese clusters, reducing thus their crystallite size and increasing their dispersion on the catalyst's surface.

4.3. Infrared spectra

The data of IR spectra indicate that Mn^{3+} and Zn^{2+} ions are occupied on tetrahedral and octahedral sites by increasing the calcination temperature. Moreover, the calcination temperature increases the area and intensity of the investigated bands due to the increase in the amount of zinc manganite produced. In addition, the difference in the position and the area of the bands is referred to the formation of more $ZnMn_2O_4$. The crystalline bulk form of $ZnMn_2O_4$ is a normal spinel with Zn^{2+} ions only on the A sites and Mn^{3+} ions only on the B sites. On the basis of the above data the zinc manganite compound has a normal spinel structure and the cation distribution is $(Zn^{2+})_A[Mn^{3+}]_BO_4^{2-}$.

4.4. Morphology studies

Transmission electron micrographs of pure Z_1M_2 and doped $L_1Z_1M_2$ and $L_4Z_1M_2$ mixed oxides and treated at 400, 600 and 800 °C brought about a significant increase in the particle size of the investigated solids. Particles indicating the important role in preparation of the nanosized zinc manganite.

4.5. DSC and TGA studies

The differential scanning calorimetry analysis, DSC, curves of pure Z_1M_2 and doped $L_1Z_1M_2$ and $L_4Z_1M_2$ mixed oxides were examined. The first sets correspond to desorption of the physisorbed water and water crystallization of different precursors. The second and third sets referred to different steps of decomposition of zinc and manganese carbonates and also lithium nitrate. The fourth sets of peaks for pure and doped mixed solids might indicate the solid-solid interaction between the thermal products of Zn/Mn mixed solids and/or phase transformation process of one the produced products. Moreover, an additional exothermic peak was observed in DSC curves of doped mixed solids and located at 790–820 °C. This sharp and weak peak might be attributed to solid state reaction between Li_2O and Mn_2O_3 yielding $LiMnO_2$ phase. These findings were confirmed by XRD measurements.

The thermo-gravimetric, TG and DTG, curves of the pure solid and those treated by doping with 1 and 4 mol% Li_2O, indicated that the first peaks correspond to desorption of crystallized water of the mixed solid and decomposition of basic zinc carbonate. The second peak indicated the thermal decomposition of manganese carbonate to produce Mn_2O_3. The difference between the observed value (21.8%) and that calculated experimentally (24%) might indicate the formation of $ZnMn_2O_4$ phase due to the solid state reaction between Zn and Mn oxides as in Table 4. This speculation was

Table 4
Quantitative calculations for the TGA data of Z_1M_2.

Mixed oxides	Temperature range (°C)	Removed species	Wt. loss (%) theoretical	Wt. loss (%) calculated
Pure $ZnCO_3{\cdot}Zn(OH)_2$ $2MnCO_3$	261	$0.5H_2O$, $0.5CO_2$	10.77	9.4
$ZnO{\cdot}2MnCO_3$	433.5	$2CO_2$	21.02	24

Table 5
Reaction rate constant per unit mass ($k \times 10^{-3}$ min^{-1} g^{-1}) for the catalytic decomposition of H_2O_2 decomposition over pure Z_1M_2 and doped Z_1M_2–Li_1, Z_1M_2–Li_4 systems prepared by mechanical mixing method being calcined at 400, 500, 700 and 800 °C.

Sample	$k \times 10^{-3}$ (min^{-1} g^{-1})			
	Calcination temperature	30 °C	40 °C	50 °C
Pure Z_1M_2 oxide	400	9.96	18.3	27.05
	500	20.24	34.7	50.44
	700	7.82	10.58	13.32
	800	2.79	5.2	8.24
Doped $L_4Z_1M_2$ oxide 4 mol%	400	9.03	10.76	15.71
	500	9.95	14.12	19.44
	700	3.8	6.04	8.39
	800	2.31	3.67	4.85
Doped $L_1Z_1M_2$ oxide 1 mol%	400	8.05	9.38	10.14
	500	8.71	9.55	13.82
	700	2.67	3.29	9.07
	800	2.36	2.62	3.7

confirmed by XRD measurments [22,23]

$$2MnCO_3 + 0.5ZnCO_3{\cdot}Zn(OH)_2 \rightarrow 2MnCO_3 + ZnO + 0.5H_2O + 0.5CO_2$$

$$2MnCO_3 + ZnO + 0.5O_2 \rightarrow ZnO + 2CO_2 + Mn_2O_3$$

$$ZnO + Mn_2O_3 \rightarrow ZnMn_2O_4$$

4.6. Catalytic activity

The catalytic activity of pure Zn/Mn oxide reflects the effect of calcination temperatures and dopant concentrations. It is seen from Table 5 that the k values of the catalyzed reaction calcined at 400, 500, 700 and 800 °C.

At 400 exhibits highest catalytic activity, increase of the calcination temperature at 600 °C resulted in a decrease in the catalytic activity. Further decrease was found by increasing the calcination temperature up to 800 °C.

From the results of XRD of the pure and doped mixed solids preheated at 400, 600 and 800 °C, it can be suggested that the catalytic activity at 400 and 600 °C might be attributed to the presence of Mn^{4+}/Mn^{3+} and Zn^{2+}/Zn, Mn^{3+}/Zn^{2+} ion pairs [24]. By increasing the treatment up to 800 °C, the activity was sharply decreased. This might be attributed to the increase of the degree of crystallinity of the oxides with subsequent formation $ZnMn_2O_4$ precursors [25]. However, the pure and doped mixed solids precalcined at 1000 °C did not show any measurable catalytic activity. This might be attributed to the formation of inactive spinel compound [26] such as $ZnMn_2O_4$, Mn_3O_4 and/or sintering process [27]. The compounds containing lithium were found to have catalytic activity less than those without lithium (Table 5). This may be attributed to the probability of the solid reaction between lithium oxide and manganese oxide leading to the formation of the less active lithium manganese oxide, according to the following equation:

$$Li_2O + Mn_2O_3 \rightarrow 2LiMnO_2$$

The increase of lithium content leads to more decrease in the catalytic activity. From the above results, it can be concluded that the change in the catalytic activity of pure and doped mixed solids calcined at different temperatures might be attributed to the change in the oxidation states of the active contents involved in the catalytic system.

5. Conclusions

- The particle size of the whole prepared samples in all phases is found to be ranging from 36 to 88 prepared manganese and zinc oxide.
- Crystalline ZnO, Mn_2O_3 and $ZnMn_2O_4$ phases were detected for pure Zn/Mn oxide and $ZnLiO_2$ also found for LiO_2-doped Zn/Mn mixed solids thermally treated at temperatures between 400 and 1000 °C.
- The surface concentration of Mn in all solids was higher than Zn determined by EDX.
- The migration of Mn atoms from surface into bulk was observed while the number of Zn atoms on the surface of sample was increased when the sample was thermally treated from 600 up to 800 °C then decreased by treatment the sample at 1000 °C.
- For the doped samples the migration of Mn atoms from the bulk to the surface was detected while the number of Zn atoms on the surface of sample was decrease when the sample was thermally treated from 600 up to 800 °C then increased by increasing the sample at 1000 °C.
- The catalytic activity increased with increasing reaction temperature reaching a maximum at 600 °C then decreased for catalysts thermally treated at 800 °C. The calcination of solids at 1000 °C showed no detectable catalytic activity in H_2O_2 decomposition.
- Catalysts containing lithium were found to be less active than that without lithium. This explained by the fact that lithium may react with manganese oxide forming the less active lithium manganites.

References

[1] T. El-Nabarawy, A.M. Youssef, S.A. Sayed, Adsorp. Sci. Technol. 19 (2001) 159.
[2] S.W. Donnea, A.F. Hollenkampb, B.C. Jones, J. Power Sources 195 (2010) 367–373.
[3] I.N. Demchenko, K.L. Jablonskac, T. Tyliszczak, N.R. Birkner, W.C. Stolte, M. Chernyshov, O. Hemmers, J. Electron Spectrosc. Relat. Phenom. 171 (2009) 24–29.
[4] C. Jonesa, J. Kieran, S. Colea, H. Taylor, M.J. Crudaceb, G.J. Hutchings, J. Mol. Catal. A: Chem. 305 (2009) 121–124.
[5] N.M. Deraz, Colloids Surf. A 190 (2001) 251.
[6] W. Zhang, L. Jiangying, X.M. Dua, Z. Zhang, Mater. Res. Bull. 44 (2009) 2072–2080.
[7] R.S. Mikhail, T. El-Nabarawy, A.M. Youssef, Surf. Technol. 11 (1980) 279.
[8] J. Deren, J. Raber, J. Steichowski, Proceedings of the 3rd International Congress on Catalysis, Amsterdam, vol. 2, 1964, p. 39.
[9] N.M. Deraz, Chin. J. Catal. 29 (8) (2008) 687–695.
[10] N.M. Deraz, H.H. Salim, A. Abd El-Aal, Mater. Lett. 53 (2002) 102.
[11] R. Chitrakar, S. Kasaishi, A. Umeno, K. Sakane, N. Takagi, Y.S. Kim, K. Ooi, J. Solid State Chem. 169 (2002) 35–43.
[12] W.M. Shaheen, N.M. Deraz, M.M. Selim, Mater. Lett. 52 (2002) 130.
[13] N.M. Deraz, Thermochim. Acta 401 (2003) 175–185.
[14] N.M. Deraz, Thermochim. Acta 421 (2004) 171.
[15] R.L. Chin, D.M. Hercules, J. Catal. 74 (1982) 121.
[16] N.M. Deraz, J. Anal. Appl. Pyrolysis 82 (2008) 212.
[17] S.B. Kanungo, Indian J. Chem. A 26 (1987) 373.
[18] J. Deren, J. Raber and J. Steichowski, Proc. 3rd Int. Congr. Catal. Amsterdam 2 (1964) 39.
[19] L.S. Puckhaber, H. Cheung, D.L. Cocke, A. Clearfield, Solid State Ionics 32 (1989) 206.
[20] W.M. Shaheen, M.M. Selim, Thermochim. Acta 322 (1998) 117.
[21] T.L. Webb, H. Heystek, The Differential Thermal Investigation of Clays, Mineralogical Society, London, 1957.
[22] S. Brönauer, L.S. Deming, W.E. Deming, E.E. Teller, J. Am. Chem. Soc. 62 (1723) 1940.
[23] M.M. Selim, M.K. El-Aiashy, 21(1994) 265.
[24] T. Farid, Z.A. Omran, M.M. Selim, Bull. NRC Egypt 20 (1995) 129.
[25] R. Metz, J.P. Caffin, R. Lergros, A. Rousset, J. Mater. Sci. 24 (1989) 83.
[26] V. Mucka, Collect. Chem. Common. 49 (1984) 1.
[27] V.A. Sadykov, P.G. Tsyrul'nikov, Kinet. Katal. 18 (1977) 137.